

Possible reaction pathways of the acetamiprid molecule according to the DFT calculation method

B. Eren¹, Y. Yalcin Gurkan^{2*}

¹Namik Kemal University, Faculty of Agriculture, Tekirdag, Turkey

²Namik Kemal University, Department of Chemistry, Tekirdag, Turkey

Received July 1, 2018; Accepted October 1, 2018

Acetamiprid, the major active ingredient of some pesticides, is a subclass of the neonicotinoid group and is used especially against whitefly, aphididae, leaf bugs, potato bugs which affect products such as cotton, tobacco, potato, tomato, nut, citrus, planted in greenhouses and fields. Quantum chemical calculations of density functional theory (DFT) were used to investigate the structural and physical characteristics of acetamiprid. The analysis was made on the probable reaction path of acetamiprid molecule with OH radicals. The calculation of the optimized geometry and the geometric optimization for determination of the lowest energy status were made by the Gauss View 5 and the Gaussian 09 program. Activation energy for the probable reaction paths was calculated and its most stable states from the thermodynamic perspective were determined for the different phases. The aim of this study is to estimate the degradation mechanism of acetamiprid molecule in gaseous phase, in ethanol and water as polar solvents, and in chloroform as a partially polar solvent, all of which were analysed through the conductor-like screening solvation model (COSMO) as the solvation model. The probable reaction path of the activation energy was calculated, and its most stable state in the thermodynamic frame was determined for these phases.

Keywords: Acetamiprid, DFT, Pesticide

INTRODUCTION

Recently, chemical treatments are widely used for high fertility in agricultural fields. These chemicals are used for the combat with insects, fungi, flies, disease agents, and weeds. Pesticides are beneficial when used at proper amounts and time whereas their improper use in terms of excess and improper time results in problems in human health, as well as in the increase of environmental pollution beside its negative effect on other livings. Pesticides are known to be highly poisonous but still are widely used in great amounts in agriculture. Thus, it is obvious that pesticides are extremely dangerous in both use and production.

In developing countries, mortality caused by pesticide poisoning, suicide attempts due to the easy accessibility of pesticides on the market, the occurrence of leucemias, urinary bladder or pancreatic cancers, as well as lymphomas due to pesticides have been reported widely in researches carried out recently. Moreover, it has also been reported that there has been an increase in congenital disorders in children of parents exposed to pesticides. The use of the same pesticides in great amounts throughout many years caused many pest populations to desensitise and become resistant to these chemicals. Therefore, it is essential that insecticides be renewed continuously. As a result, the use of organochlorine and organophosphorous

insecticides has been reduced in time, pyrethroides have been used as an alternative, and later the use of neonicotinoids has progressively increased [1-8].

There are many ways for organic contaminants to enter the environment. The excessive use of insecticides including organic contaminants leads to residuals of these compounds at high levels. The cycle starts with soil, ground and surface waters, then with fruits and vegetables regardless of their being fresh or processed, and finally reaches the human beings through consumption [9,10].

Acetamiprid, being an odorless neonicotinoid insecticide, is an organic compound with the chemical formula $C_{10}H_{11}ClN_4$. As stated in many studies, organic contaminants are known to exist in water at very low concentrations. Thus, it is crucial that drinking water be purified from the organic contaminants. Solar light on earth provides natural purification of water systems such as pools, lakes, creeks, and rivers. Large organic molecules are degraded into smaller basic molecules through sunbeams, and finally form CO_2 , H_2O , NH_4^+ and other small molecules [11-13].

OH radical acts like an electrophile in its reaction with any organic molecule and therefore readily attacks the unsaturated bonds, while O radical is a nucleophile, and thus does not attack these bonds. If there is an aliphatic side chain readily bound to an aromatic molecule, radical H attacks O, whereas OH radical preferentially attacks

* To whom all correspondence should be sent:

E-mail: yyalcin@nku.edu.tr

the aromatic ring, which can result in the formation of various products when pH reaches a range in which O radical is the reactant rather than OH radical. Hydroxyl radical, known to be the most reactive type in biological systems, goes into reaction with every biomolecule it confronts, including water. Potentially, every biomolecule is a hydroxyl radical scavenger at different speeds. Aromatic compounds are good detectors since they hydroxylate. In addition, the position of attack to the ring depends on the electron withdrawal and the repulsion of previously present substituents. The attack of any hydroxyl radical to an aromatic compound results in the formation of a hydroxylated product [13-16].

This study was conducted in order to find out whether this molecule, being named D molecule in our study, would be fragmented in the nature under the formation of small molecules. The kinetics of the degradation reaction path of D molecule with OH radical was theoretically analysed through the density functional theory (DFT) method.

COMPUTATIONAL SET-UP AND METHODOLOGY

Computational models

The models of the molecules were formed by the use of the mean bond distances and the geometric parameters of the closed ring. Tetrahedral angles were used for the sp^3 -hybridized carbon and oxygen atoms and 120° for the sp^2 -hybridized carbon atoms was used in the computational modelling. The aromatic ring was left planar, excluding the position of attack. Due to the change in the hybridization state of the carbon at the addition centre from sp^2 to sp^3 , the attacking $\bullet OH$ was presumed to create a tetrahedral angle with the C-H bond [17].

Molecular orbital calculations

In photocatalytic degradation reactions of the D molecule it is possible that products more harmful than those in the original material could be formed. Therefore, before experimentally realizing a photocatalytic degradation reaction, it is essential to know the nature of the primary intermediate products. The most reliable and accurate information is gathered through calculations realized with quantum mechanical methods. Thus, since the yield produced was the same, photocatalytic degradation reactions of the D molecule and its hydroxy derivatives are based on the direct reaction of these molecules with $\bullet OH$.

With this aim, the kinetics of the reactions of the D molecule with $\bullet OH$ were theoretically analysed.

The study was initiated with the D molecule which was then exposed to reaction with $\bullet OH$ and the reaction yields were modelled in different phases. Experimental results in the scientific literature showed that $\bullet OH$ detaches a hydrogen atom from saturated hydrocarbons, and $\bullet OH$ is added to unsaturated hydrocarbons and materials with this structure [18,19]. For this purpose, all reaction paths for the analysed reactions were determined. For these fragmentation paths, molecular orbital calculations of the D molecule were performed with the density functional theory (DFT), their molecular orbital calculations were realized and their geometries optimized. In order to explore the conformational landscape of the molecules, a potential energy surface scan was performed along the torsional coordinates mentioned above in a relaxed manner. The scan was calculated using the B3LYP/6-31G* method [20].

Kinetic data treatment

The aim of this study was to develop a model providing the outcome of the photocatalytic degradation reactions. The vibration frequencies, the thermodynamic and electronic features of every structure were calculated using the obtained optimum geometric parameters.

Subsequently, based on the quantum mechanical calculation results, the rate constant and activation energy (E_a) of every reaction was calculated at a temperature of $25^\circ C$. In order to enable the calculation of the rate constant, it is necessary initially to calculate the partition function of the activated complex. To realize this calculation, it is essential to know the geometry of the complex and the moments of inertia. In addition, E_a should be known in order to determine the rate constant. The activation energy, as the vibration frequency, can only be calculated quantum mechanically. The optimized geometric structures were drawn *via* GaussView 5, and the calculations were realised within the Gaussian 09 programme packet [20].

Methodology

The investigated reaction system was composed of $\bullet OH$, which are open-shell species. It is known that open-shell molecules cause severe problems in quantum mechanical calculations. The self-consistent field method (SCF) calculation will proceed for an open-shell case in the same way as for a closed-shell case. However, since two sets of equations have to be dealt with, at each iteration, the program has to consider, either simultaneously or successively, the closed-shell and the open-shell equations. In this respect, the computational burden could be two-times larger for an open shell than

that for a closed-shell. Another point raised in connection with the optimization of the SCF process for open-shell molecules is the relative intricacy of the sequence of calculations for the closed-shell Hamiltonian and the open-shell Hamiltonian [21].

DFT methods, taking the electron correlation into account, use the precise electron density to calculate molecular properties and energies. Spin contamination does not affect them and hence, for calculations involving open-shell systems, they become favourable. DFT calculations were made by the hybrid B3LYP functional combining the HF and Becke exchange terms with the Lee–Yang–Parr correlation functional. It is essential in such calculations to choose the basis set. Based upon the obtained results, optimization in the current study was carried out at the B3LYP/6-31G(d) level [13,20].

Solvent effect model

The energetics of the degradation reactions of all organic compounds are affected by water molecules in aqueous media. In addition, geometry relaxation on the solutes is induced by H₂O. Solvation is based on the affinity between molecules. In order to be able for a solvent to solve a substance, affinity between the solvent and molecules of the solute has to be greater than the affinity between the solvent and the own molecules of the solute. Generally, solvation occurs in situations where solvent and solute have the same construct. If a molecule consists of different atoms, the affinity of each atom towards electrons is different. As a result, there is an electron surplus; therefore partial negative load in part of the molecule, and there is lack of electrons; therefore partial positive load in the remaining part of the molecule. These kinds of molecules are called polar molecules. If the conditions mentioned above do not exist; in other words, they do not reveal any polarization, these are called apolar molecules [22].

C-H and C-C bonds of the ethanol molecule are apolar, whereas its O-H and C-O bonds are polar. Thus, since one end reveals polar, and the other reveals apolar characteristics, ethanol is a good solvent for both polar and apolar substances. Chloroform is a heavy, colourless liquid solvent that is slowly oxidised under the influence of light, and can evaporate easily. Beside being a partially polar solvent, chloroform, or trichloromethane was chosen to be the solvent for our molecule because of its partial negative loaded ends of the chlorine atoms.

On the other hand, it was indicated in previous studies that there is an insignificant effect of

geometry changes on the energy of the solute for both open- and closed-shell structures [23].

In this study, DFT/B3LYP/6-31+G(d) calculations were realised for the optimized structures of the reactants, the pre-reactive and the transition state complexes and the product radicals, by using the COSMO (conductor-like screening solvation model) as the solvation method in order to consider the effect of H₂O on the energetics and the kinetics of D molecule reactions with •OH. Water at 25 °C was used as a solvent with dielectric constant, $\epsilon = 78.39.28$

The COSMO method explains the solvent reaction field through apparent polarization charges distributed on the cavity surface, determined by presuming that the total electrostatic potential cancels out at the surface. The solvation in polar liquids can be described by this condition. Therefore, this method was chosen to be appropriate for the present study [24].

RESULTS AND DISCUSSION

As seen from different angles in an optimized form, lincomycin molecule (D) has a conformation far from a planar structure in terms of geometric shape (Fig. 1).

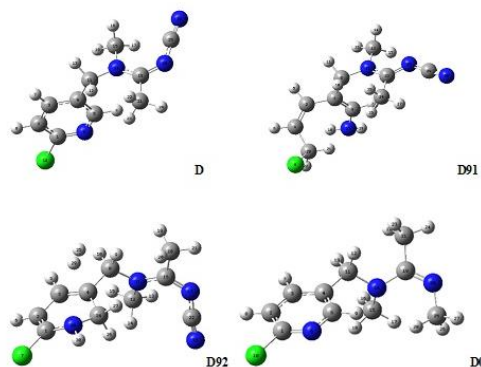


Figure 1. Optimized figures of the D molecule and its three stable fragments D91, D92, and D0. (Grey, C; green, Cl; white, H; blue, N)

Reaction centres can be explained through Mulliken charge distribution of the molecule. According to the data in Table 1, the degradation reaction occurred due to the electronegativity of Cl, and N.

When Mulliken charges of the D molecule are analysed, N₆, N₁₅, N₂₀ and N₂₆ are determined to be atoms with high electronegativity. Various fractions were obtained through fragmentation from bonds close to these atoms.

The molecule was analysed whether stable fractions found through the analysis of bond lengths and angles shown in Table 2 were compatible with thermodynamic values found in Table 3. In addition

to predicting that the fragmentation occurs from the electronegative atoms in molecules, bond lengths, bond lengths starting from long to short ones, bond angles and by taking into consideration the molecules are divided into fractions by stable-close ring.

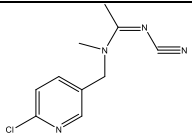
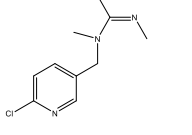
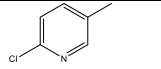
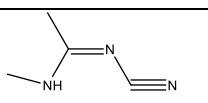
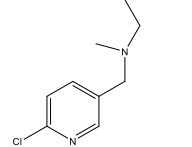
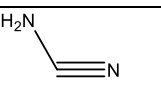
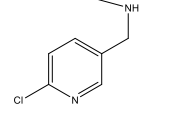
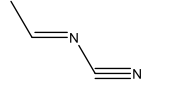
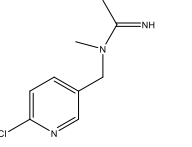
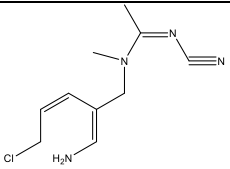
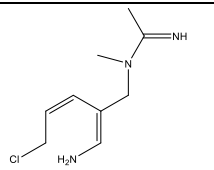
Table 1. Mulliken loads of the studied fragments

D		D0		D1		D2		D3	
C ₂	-0.122839	C ₂	-0.123041	C ₂	-0.122975	N ₁	-0.575866	C ₂	-0.224276
C ₃	-0.141567	C ₃	-0.148100	C ₃	-0.139127	C ₂	-0.316119	C ₃	-0.159563
C ₅	-0.004049	N ₆	-0.405381	C ₅	-0.015604	N ₇	-0.503063	C ₄	-0.062557
N ₆	-0.401661	Cl ₁₀	-0.009623	N ₆	-0.403007	C ₈	-0.535133	N ₆	-0.504356
Cl ₁₀	0.005156	C ₁₁	-0.212164	Cl ₁₀	-0.015134	N ₁₃	-0.499836	Cl ₁₀	0.002413
C ₁₁	-0.239135	N ₁₄	-0.426162	C ₁₁	-0.535898			C ₁₁	-0.129139
N ₁₅	-0.403753	C ₁₅	-0.317742					N ₁₄	-0.569425
C ₁₅	-0.342771	N ₂₀	-0.405623					C ₁₅	-0.294353
N ₂₀	-0.504061	C ₂₁	-0.510021					C ₁₉	-0.481934
C ₂₁	-0.536110	C ₂₅	-0.335521					C ₂₃	-0.114721
N ₂₆	-0.493369								
D4		D5		D6		D7		D8	
N ₂	-0.446855	C ₂	-0.123412	N ₂	-0.394345	C ₂	-0.122372	N ₂	-0.358128
N ₃	-0.752971	C ₃	-0.149817	C ₃	-0.506851	C ₃	-0.149256		
		N ₆	-0.406789	N ₈	-0.452780	N ₆	-0.404164		
		Cl ₁₀	-0.017616			Cl ₁₀	-0.007115		
		C ₁₁	-0.213183			C ₁₁	-0.222627		
		N ₁₄	-0.534391			N ₁₄	-0.404996		
		C ₁₅	-0.310549			C ₁₅	-0.340831		
						N ₂₀	-0.628160		
						C ₂₁	-0.522725		
D91		D92		D10		D11		D12	
C ₁	-0.158579	C ₂	-0.277066	C ₂	-0.123495	C ₂	-0.136641	N ₂	-0.450958
C ₂	-0.211035	C ₃	-0.170426	C ₃	-0.148966	C ₃	-0.150912	C ₃	-0.511351
C ₃	-0.094373	C ₄	-0.002703	N ₆	-0.406735	N ₆	-0.403561	N ₈	-0.467603
Cl ₈	-0.110206	Cl ₇	0.017264	Cl ₁₀	-0.017595	C ₁₀	-0.242085	C ₉	-0.522648
C ₉	-0.117457	C ₈	-0.180448	C ₁₁	-0.210702	N ₁₃	-0.399893		
N ₁₂	-0.671279	N ₁₁	-0.661729	N ₁₄	-0.715092	C ₁₄	-0.341379		
C ₁₃	-0.276052	C ₁₂	-0.310825			N ₁₉	-0.507336		
N ₁₇	-0.869382	N ₁₇	-0.661817			C ₂₀	-0.536669		
C ₂₀	-0.417418	C ₁₈	-0.566280			N ₂₅	-0.496034		
C ₂₄	-0.589520	N ₂₃	-0.494814						
N ₂₈	-0.683934	C ₂₄	-0.113899						
N ₃₀	-0.489022	N ₂₈	-0.750932						

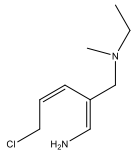
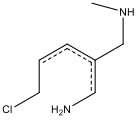
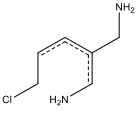
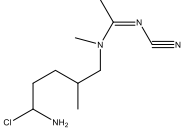
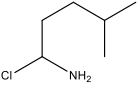
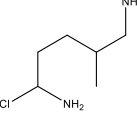
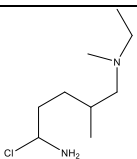
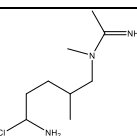
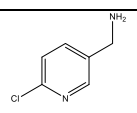
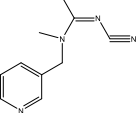
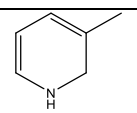
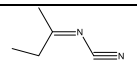
Table 2. Bond lengths and angles of stable fragments of the D molecule.

D	Bond Length	D91	Bond Length	D92	Bond Length	D0	Bond Length
C ₁ Cl ₁₀	1.75997	C ₂₉ N ₃₀	1.14137	C ₁₆ N ₁₇	1.28635	C ₁₉ N ₂₀	1.27758
C ₁ N ₅	1.31877	C ₂₉ N ₂₈	1.33081	C ₁₆ N ₁₁	1.34890	C ₁₉ N ₁₄	1.42779
C ₅ N ₅	1.34130	C ₂₃ N ₂₈	1.28942	C ₈ N ₁₁	1.46565	C ₁₅ N ₂₄	1.46504
C ₁₁ N ₁₄	1.46336	C ₂₃ N ₁₂	1.34220	C ₁₂ N ₁₁	1.46211	C ₂₅ N ₂₀	1.45043
C ₁₉ N ₁₄	1.36653	C ₁₃ N ₁₂	1.45812	C ₂₂ N ₁₇	1.33058	C ₁₁ N ₁₄	1.46205
C ₁₉ N ₂₀	1.30326	C ₉ N ₁₂	1.45292	C ₂₂ N ₂₃	1.14142	C ₁₅ N ₁₄	1.46504
C ₂₅ N ₂₀	1.32618	C ₂₀ Cl ₈	1.80507	C ₁ N ₂₈	1.37615	C ₅ N ₆	1.33903
C ₂₅ N ₂₆	1.17200	C ₄ N ₁₇	1.38821	C ₂₄ N ₂₈	1.45504	C ₁ N ₆	1.32123
D	Bond Angle	D91	Bond Angle	D92	Bond Angle	D0	Bond Angle
C ₁ N ₆ C ₅	117.47936	C ₂₃ N ₂₈ C ₂₉	120.04265	C ₁₆ N ₁₇ C ₂₂	125.39757	C ₁₉ N ₂₀ C ₂₅	121.35950
C ₁₁ N ₁₄ C ₁₉	122.32345	C ₁₃ N ₁₂ C ₂₃	118.76386	N ₁₁ C ₁₆ N ₁₇	127.56093	N ₁₄ C ₁₉ N ₂₀	124.52572
C ₁₁ N ₁₄ C ₁₅	114.47495	N ₁₂ C ₂₃ N ₂₈	117.29458	C ₈ N ₁₁ C ₁₆	123.13607	C ₁₉ N ₁₄ C ₁₅	116.24421
C ₁₅ N ₁₄ C ₁₉	122.97978	C ₉ N ₁₂ C ₁₃	117.19305	C ₈ N ₁₁ C ₁₂	114.66496	C ₁₁ N ₁₅ C ₁₄	112.54777
C ₁₉ N ₂₀ C ₂₅	128.05325	C ₉ N ₁₂ C ₂₃	123.92611	C ₁₂ N ₁₁ C ₁₆	122.15344	C ₁ N ₆ C ₅	117.32205

B. Eren, Y. Yalcin Gurkan: Possible reaction pathways of the acetamiprid molecule according to the DFT ...
Table 3. Gas phase of various fractions of the D molecule, energy, enthalpy, and Gibbs Free Energy electrochemical values within ethanol, water and chloroform solvent

D	Ethanol	Chloroform	Gas	Water	Molecule
$\Delta E(\text{Au})$	-1066.661533	-1066.657084	-1066.641435	-1066.662293	
$\Delta H(\text{Au})$	-1066.660589	-1066.656140	-1066.640491	-1066.661348	
$\Delta G(\text{Au})$	-1066.719894	-1066.715610	-1066.700286	-1066.720627	
D0	-1013.681701 -1013.680757 -1013.740041	-1013.679679 -1013.678735 -1013.738112	-1013.671802 -1013.670857 -1013.729670	-1013.682075 -1013.681131 -1013.740436	
D1	-747.093774 -747.092829 -747.133275	-747.092519 -747.091574 -747.132045	-747.087855 -747.086911 -747.127422		
D2	-320.766542 -320.765598 -320.808013	-320.762939 -320.761995 -320.804441	-320.750306 -320.749362 -320.793758	-320.767160 -320.766216 -320.808819	
D3	-916.515967 -916.515023 -916.566908	-916.514308 -916.513364 -916.565271	-916.508022 -916.507077 -916.558717	-916.516245 -916.515301 -916.567178	
D4	-148.754966 -148.754022 -148.782103	-148.752353 -148.751409 -148.779497	-148.742299 -148.741355 -148.769488	-148.755400 -148.754456 -148.782536	
D5	-841.694576 -841.693632 -841.740179	-841.692942 -841.691998 -841.738498	-841.686802 -841.685858 -841.732216	-841.694850 -841.693906 -841.740459	
D6	-226.126057 -226.125113 -226.159532	-226.123925 -226.122981 -226.157407	-226.116154 -226.115210 -226.149667	-226.126418 -226.125473 -226.159892	
D7	-974.414056 -974.413112 -974.470948	-974.411268 -974.410323 -974.465849	-974.401101 -974.400157 -974.455140	-974.414487 -974.413542 -974.469627	
D8	-93.410013 -93.409069 -93.431904	-93.408692 -93.407748 -93.430587	-93.403610 -93.402666 -93.425523	-93.410232 -93.409288 -93.432123	
D91	-1064.369962 -1064.369018 -1064.432278		-1064.353352 -1064.352407 -1064.415887	-1064.370790 -1064.369846 -1064.433133	
D91a	-972.625517 -972.624573 -972.685408	-972.622686 -972.621742 -972.680922	-972.617066 -972.616122 -972.674740	-972.626051 -972.625107 -972.685981	

B. Eren, Y. Yalcin Gurkan: Possible reaction pathways of the acetamidiprid molecule according to the DFT ...

D91b	-918.745749 -918.744805 -918.802374	-918.742527 -918.741582 -918.798706	-918.746047 -918.745103 -918.802688		
D91c	-840.747044 -840.746100 -840.797646	-840.741632 -840.740687 -840.790546			
D91d	-801.738985 -801.738041 -801.787067	-801.749466 -801.748522 -801.796536	-801.746628 -801.745684 -801.792172		
D92	-1064.361834 -1064.360890 -1064.424135	-1064.317001 -1064.316057 -1064.383316	-1064.362618 -1064.361673 -1064.424920		
D92a		-746.750810 -746.749866 -746.794447	-746.753241 -746.752297 -746.797424		
D92b	-840.597931 -840.596987 -840.653717	-840.724588 -840.723643 -840.778518	-840.667576 -840.666632 -840.713670	-840.599520 -840.598576 -840.654981	
D92c	-918.748967 -918.748023 -918.805843	-918.724593 -918.723649 -918.785350	-918.667209 -918.666265 -918.719474	-918.749241 -918.748297 -918.806614	
D92d	-972.566402 -972.565458 -972.620443	-972.598733 -972.597788 -972.661499	-972.534998 -972.534053 -972.589067	-972.567422 -972.566478 -972.621462	
D10	-802.416626 -802.415682 -802.459099	-802.414736 -802.413792 -802.457004	-802.407640 -802.406696 -802.449665	-802.420704 -802.419760 -802.462825	
D11	-607.035785 -607.034841 -607.091209	-607.054447 -607.053503 -607.109709	-607.046025 -607.045081 -607.101890	-607.055139 -607.054195 -607.110378	
D11a	-287.845853 -287.844909 -287.886376	-287.817814 -287.816870 -287.863549	-287.813317 -287.812373 -287.858430		
D12		-265.411123 -265.410178 -265.448924			

For each fraction, physicochemical calculations in gaseous phase, ethanol and water solvents which are polar, as well as in chloroform revealing partial polarity, were performed. ΔE energy, ΔH enthalpy

and ΔG Gibbs free energy values given in Table 3 are stated for each fragment separately.

Three probable stable fragmentation pathways of the D molecule are given in Figures 2, 3 and 4.

CONCLUSIONS

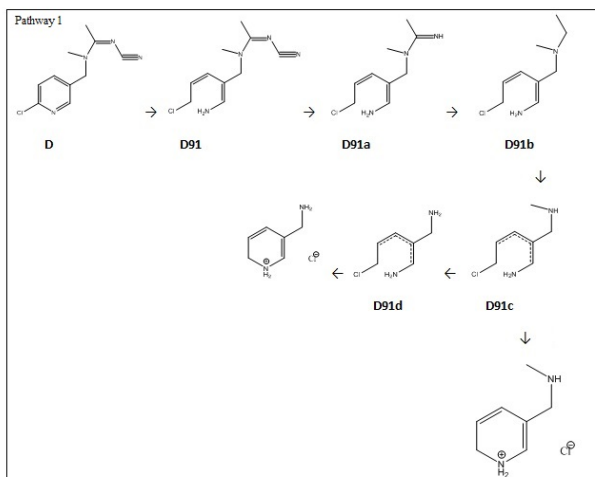


Figure 2. The assumed 1st fragmentation path of the most stable D91 fragment of the D molecule.

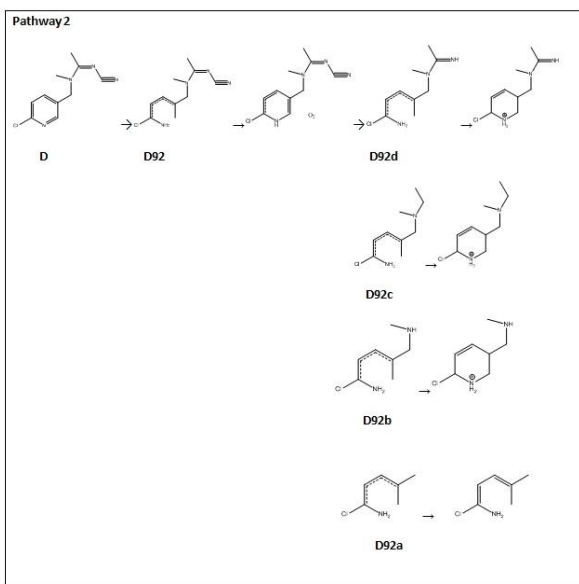


Figure 3. The assumed 2nd fragmentation path of the stable D92 fragment of the D molecule.

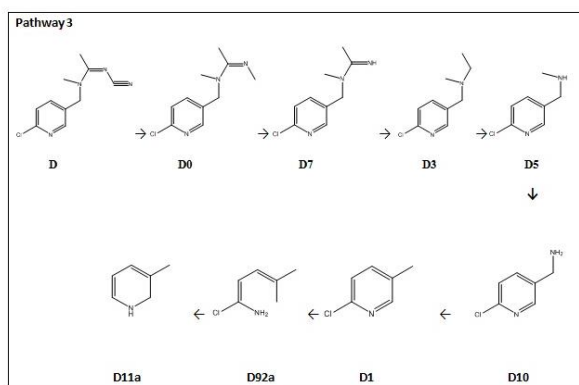


Figure 4. The assumed 3rd fragmentation path of the stable D0 fragment of the D molecule.

When ΔG Gibbs free energy values were analysed, it was seen that ΔG value of each fragmentation was negative. These results show that fragmentation occurred spontaneously. Blank parts in Table 3 indicate that fragments either were not dissolved in those solvents or became deformed. Fragments with the lowest electrochemical energy, in other words, the most stable fragments are D91 with -1064.369962 Au, D92 with -1064.361834 Au, D0 with -1013.681701 Au, and D7 with -974.414056 Au, respectively.

D91 and D92 fragments are formed through the opening of right and left bonds of N atom bound to the closed ring. As known, closed rings do not fragment voluntarily due to their being stable. In our study, more investigation was conducted to find out whether there will be closure in the further phases of these molecules due to their having the lowest energy. D92 fragment closed immediately while there was no closure observed in the D91 fragment.

Three probable stable fragmentation pathways of the D molecule are given in Figures 2, 3 and 4. In Pathway 1, fragmentation process was conducted until the ring was closed. In Pathway 2, fragmentation process proceeded from different electronegative parts of the molecule, although the ring was closed at the first fragmentation, and thermochemical values in each fragmentation were calculated. When D0 fragment is analysed as the third most stable path, and the next fragment is D7, the latter is not mentioned once again as a different fragmentation path.

When energy, enthalpy and Gibbs free energy values of each fragment of the D molecule in Table 3 were analysed regarding the studied solvents, it was observed that solvation took place in water, ethanol and chloroform. Due to water being the solvent, it is the most appropriate one. When the three probable fragmentation pathways were analysed, it was seen that the D molecule was fragmented in aqueous media up to its smallest molecules.

Acknowledgements: The authors greatly appreciate Namik Kemal University Research Foundation for financial support. Project number: NKUBAP.01.GA.18.164 The authors declare that there is no conflict of interests regarding the publication of this paper.

REFERENCES

1. A. Blair, S. H. Zahm, *Environ Health Perspect.*, **103**, 205 (1995).

B. Eren, Y. Yalcin Gurkan: Possible reaction pathways of the acetamidiprid molecule according to the DFT ...

- L. M. Brown, A. Blair, R. Gibson, G. D. Everett, K. P. Cantor, L. M. Schuman, L. F. Burmeister, S. F. Van Lier, F. Dick, *Cancer Res.*, **50**, 6585 (1990).
- B. C-H. Chiu, D. D. Weisenburger S. H. Zahm, K. P. Cantor, S. M. Gapstur, F. Holmes, L. F. Burmeister, A. Blair, *Cancer Epidemiol. Biomarkers Prev.*, **13**(4), 525 (2004).
- M. Elestondd, L. Karalliedde, N. Buckley, R. Fernando, G. Hutchinson, G. Isbister, F. Konradsen, D. Murray, J. C. Piola, N. Senanayake, R. Sheriff, S. Singh, S. B. Siwach, L. Smit, *The Lancet*, **360**, 1163 (2002).
- N. V. Kovganko, Zh. N. Kashkan, *Russian J. of Organic Chem.*, **40**(12), 1709 (2004).
- J. F. Viel, B. Chalier, *Environ. Med.*, **52**(9), 587 (1995).
- T. Zheng, S. H. Zahm, K. P. Cantor, D. D. Weisenburger, Y. Zhang, A. Blair, *JOEM*, **43**, 641 (2001).
- B. T. Ji, D. T. Silverman, P.A. Stewart, A. Blair, G. M. Swanson, D. Baris, R. S. Greenberg, R. B. Hayes, L. M. Brown, K. D. Lillemoe, J. B. Schoenberg, L. M. Pottern, A. G. Schwartz, R. N. Hoover, *Am. J. Ind. Med.*, **39**(1), 92 (2001).
- D. Sharma, A. Nagpal, Y. B. Pakade, and J.K. Katnoria, *J. Environ. Res. Develop.*, **82**(4), 1077 (2010).
- E. Taillebois, Z. Alamiddine, C. Brazier, J. Graton, A.D. Laurent, S.H. Thany, J-Y. L. Questel, *BMC*, **23**, 1540 (2015).
- K. Verschueren, *Handbook of Environmental Data on Organic Chemicals*, 2nd ed., Wiley, New York, 1996.
- R. W. Matthews, D. Ollis, H. Al-Ekabi, Elsevier, New York, 1993, 121.
- B. Eren, Y. Yalcin Gurkan, *JSCS*, **82**(3), 277 (2017).
- V. G. Buxton, L. C. Greenstock, P. W. Helman, A. B. Ross, *Journal of Physical and Chemical Reference Data*, **17**, 513 (1988).
- M. Anbar, P. Neta, *Int. J. Appl. Radiat. Isot.*, **18**, 493 (1967).
- B. Halliwell, M. Grootveld, J. M.C. Gutteridge, *Methods Biochem. Anal.*, **33**, 59 (1998).
- A. Hatipoglu, D. Vione, Y. Yalcin, C. Minero, Z. Cinar, *Journal of Photochemistry and Photobiology A*, **215**, 59 (2010).
- P. W. Atkins, *Physical Chemistry*, 6th ed., Oxford University Press, New York, 1998
- K. Mierzejewska, J. Trylska, J. Sadlej, *J. Mol. Model.*, **18**, 2727 (2012).
- Gaussian 09, Revision B.04, Gaussian Inc., Pittsburgh, PA, 2009.
- H. F. Diercksen Geerd, B. T. Sutcliffe, A. Veillard, *Computational Techniques in Quantum Chemistry and Molecular Physics. Proceedings of the NATO Advanced Study Institute, Ramsau, Germany. 1974*, p. 4.
- T. W. Graham Solomons, B. Fryhle Craig, *Organic Chemistry*, 7th ed., Wiley, 1999.
- P. W. Atkins, R. S. Friedman, *Molecular Quantum Mechanics*, 4th ed., Oxford University Press Inc., New York, 2005.
- I. N. Levine, *Quantum Chemistry*, 2nd ed., Academic Press, Waltham, MA, 1993.

ВЪЗМОЖНИ РЕАКЦИОННИ ПЪТИЩА НА МОЛЕКУЛАТА НА АЦЕТАМИПРИД ПО DFT ИЗЧИСЛИТЕЛНИЯ МЕТОД

Б. Ерен¹, Я. Ялджин Гуркан^{2*}

¹ Университет Намик Кемал, Селскостопански факултет, Текирдаг, Турция

² Университет Намик Кемал, Департамент по химия, Текирдаг, Турция

Постъпила на 1 юли, 2018 г.; приета на 1 октомври, 2018 г.

(Резюме)

Ацетамиприд, основният активен ингредиент на някои пестициди, е подклас на неоникотиноидната група и се използва предимно срещу бяла муха, *aphididae*, листни бръмбари и картофени бръмбари, атакуващи продукти като памук, тютюн, картофи, домати, орехи и цитрусови плодове, отглеждани в парници и на полето. Квантово-химични изчисления с помощта на функционалната теория на плътността (DFT) са използвани за изследване на структурните и физични характеристики на ацетамиприда. Анализирани са възможните реакционни пътища на молекулата на ацетамиприда с ОН радикали. Изчисляването на оптимизираната геометрия за определяне на състоянието на най-ниска енергия е проведено чрез Gauss View 5 и програмата Gaussian 09. Изчислена е активиращата енергия на вероятните реакционни пътища и нейното най-стабилно състояние за различните фази от термодинамична гледна точка. Целта на настоящото изследване е да се определи механизъмът на разлагане на молекулата на ацетамиприда в газова фаза, в етанол и вода като полярни разтворители и в хлороформ като частично полярно разтворител. Анализите са проведени с използване на проводящия солватационен скрининг модел (COSMO). Изчислен е вероятният реакционен път на активационната енергия и е определено нейното най-стабилно състояние за тези фази от термодинамична гледна точка.